Laboratoire d'Annecy de Physique des Particules

ATLAS EXPERIMENT

10/01/2021

Measurement of the Higgs Simplified Template Cross Sections using H→γγ decays with the ATLAS experiment

Luca Franco
(on behalf of the ATLAS collaboration)

Introduction

- Measurements with Higgs to diphoton decays:
  - Total cross section;
  - Cross section in 5 production modes;
  - **Simplified Template Cross Sections (STXS).**
- Full LHC Run 2 dataset: 139 fb^{-1} of p-p collisions at $\sqrt{s}$=13 TeV;
- Results made public by the ATLAS collaboration in ATLAS-CONF-2020-026.

Simplified Template Cross Sections

- Measurements performed in the bins proposed by the STXS stage 1.2 framework:
  - Minimize theoretical uncertainties;
  - Maximize experimental sensitivities;
  - Separately measure regions of phase space potentially sensitive to BSM effects;
  - Better combine with other decay channels.

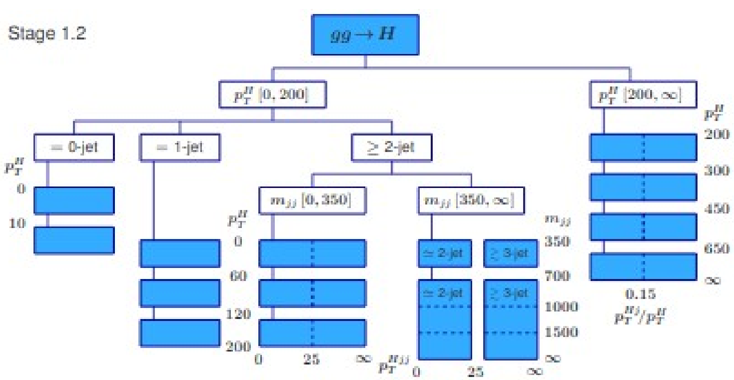

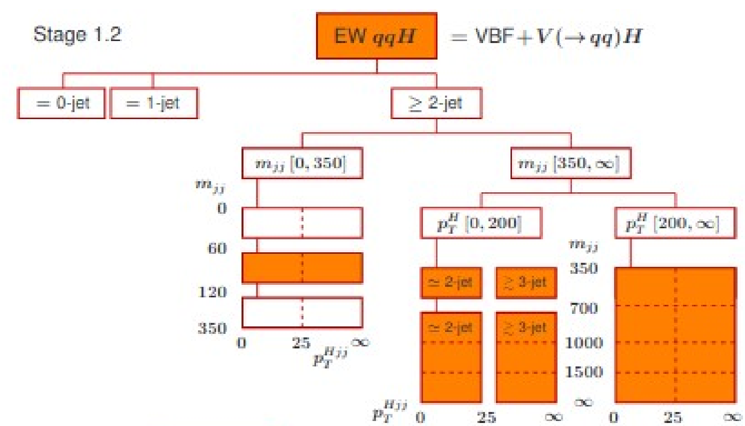

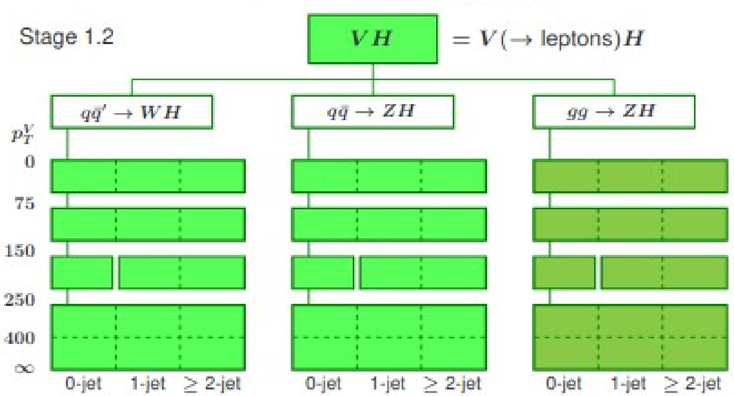

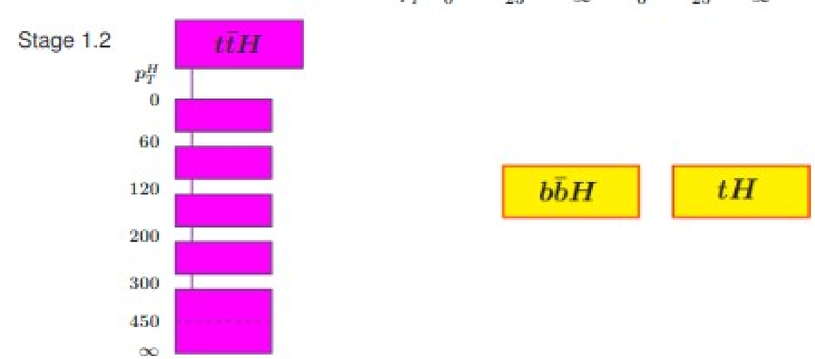

Analysis strategy

1) Select events with two photons compatible with the decay products of a Higgs boson;

2) Classify the reconstructed events in categories following STXS definition as much as possible;

3) Additional selection to separate signal from continuum background;

4) Build the signal and background models using analytic functions in each category;

5) Simultaneously fit the $m_{\gamma\gamma}$ distribution using the built signal+background model in each category;

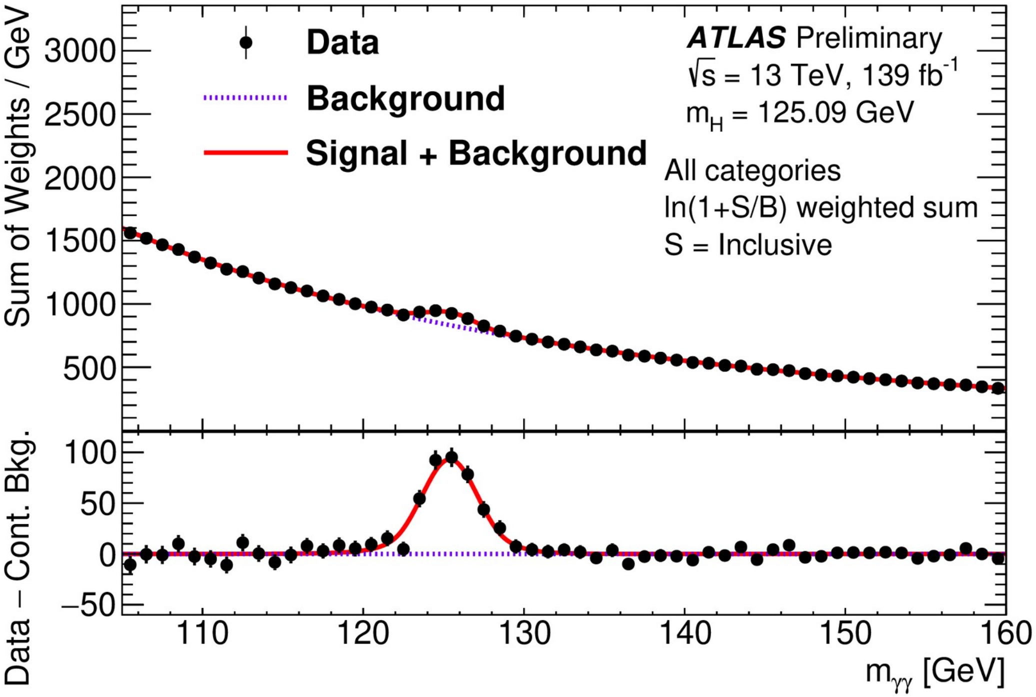

- The parameters-of-interest (POIs) are $\sigma_i \times BR_{\gamma\gamma}$ normalized to the SM prediction;

- The systematic uncertainties enter the fit through constrained nuisance parameters.

Categorization: multi-class step

- Selected events are classified into mutually exclusive categories, each targeting a STXS bin;
- Monte Carlo (MC) samples of signal processes are used to train a multiclass Boosted Decision Tree (BDT);
- Input features are variables describing the kinematic and identification properties of the reconstructed particles in the event;

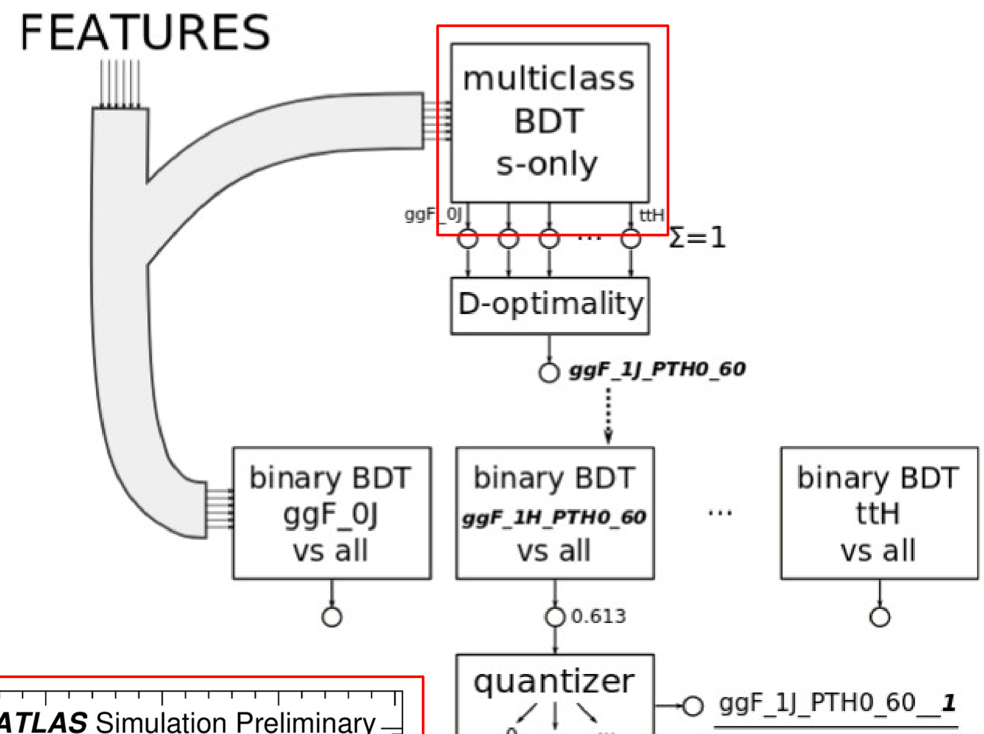

- Selection on the multi-class BDT outputs to optimise the STXS errors and correlations (D-Optimality);
- At this stage, 44 Reco categories are defined, one per STXS bin.

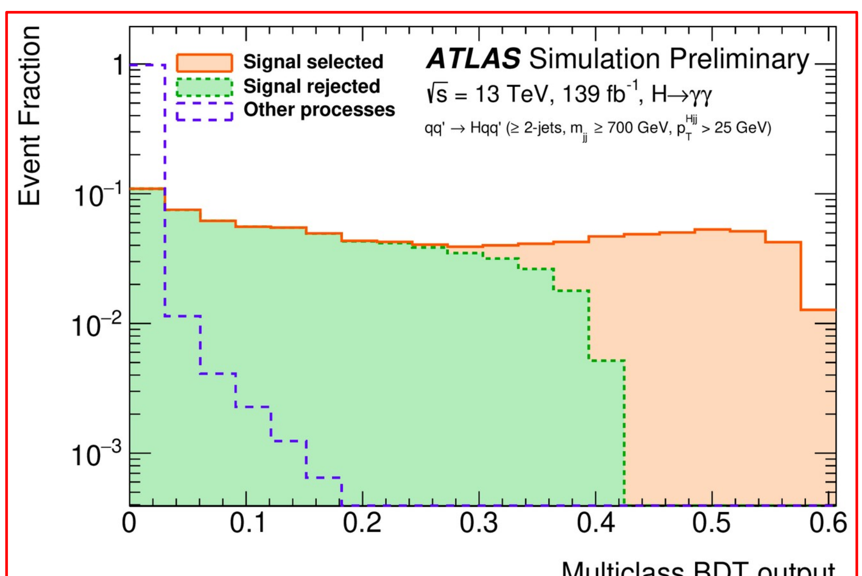

L. Franco
(CNRS-LAPP)
Epiphany 2021

Categorization: binary-class step

- Each reco category is further divided into multiple categories based on a binary BDT classifier.
- This binary BDT is trained to separate signal from continuum background in each class;
- Input features are variables describing the kinematic and identification properties of the reconstructed particles in the event;
- Finally, 88 reco categories are built and are used in the analysis.

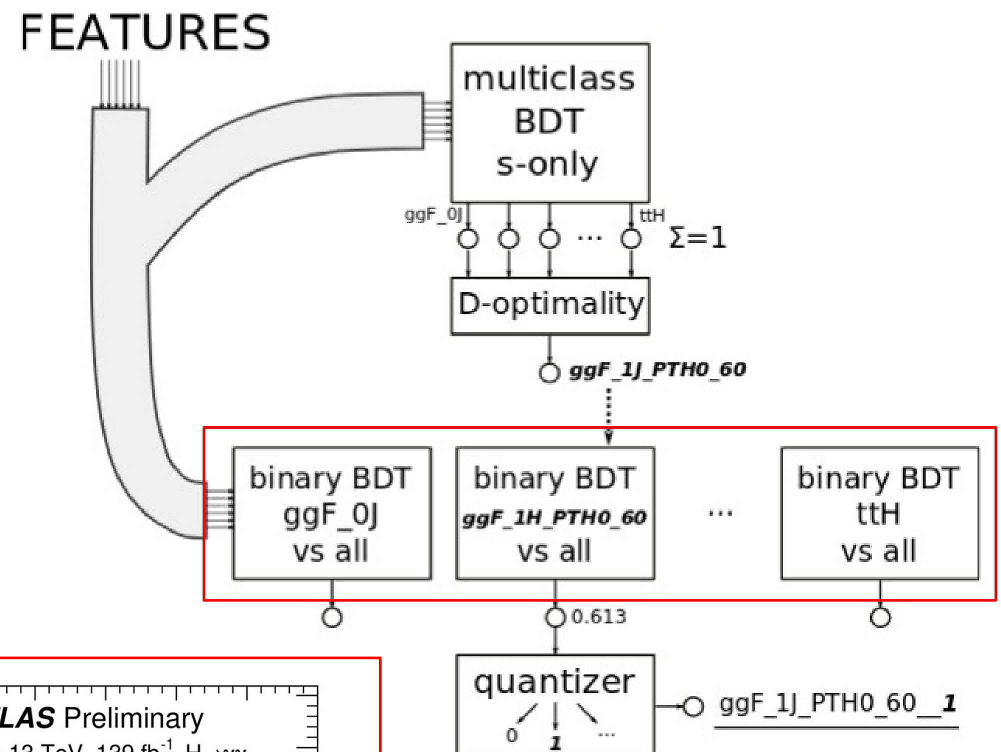

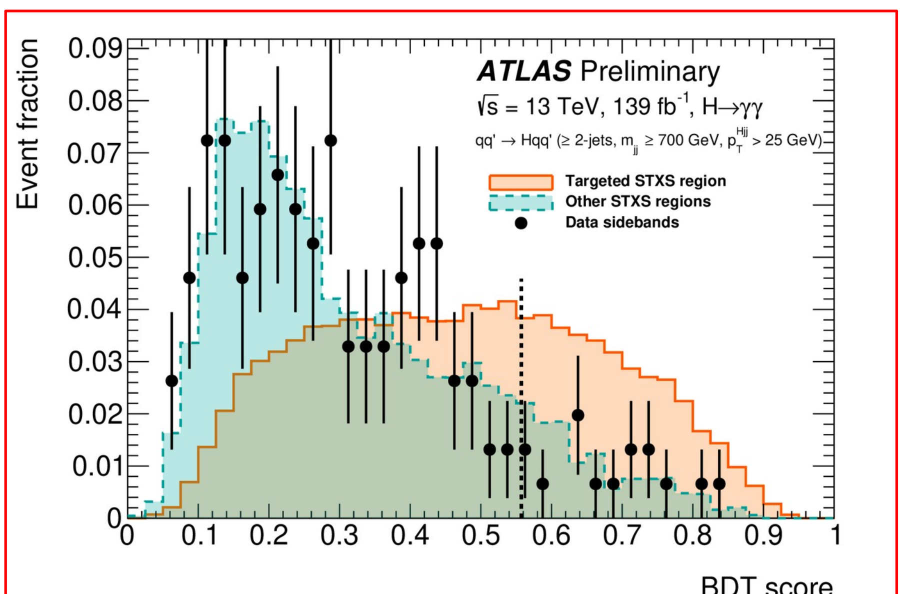

Categorization purity

- Showing correspondence between 44 truth STXS targets and 88 reconstructed categories.

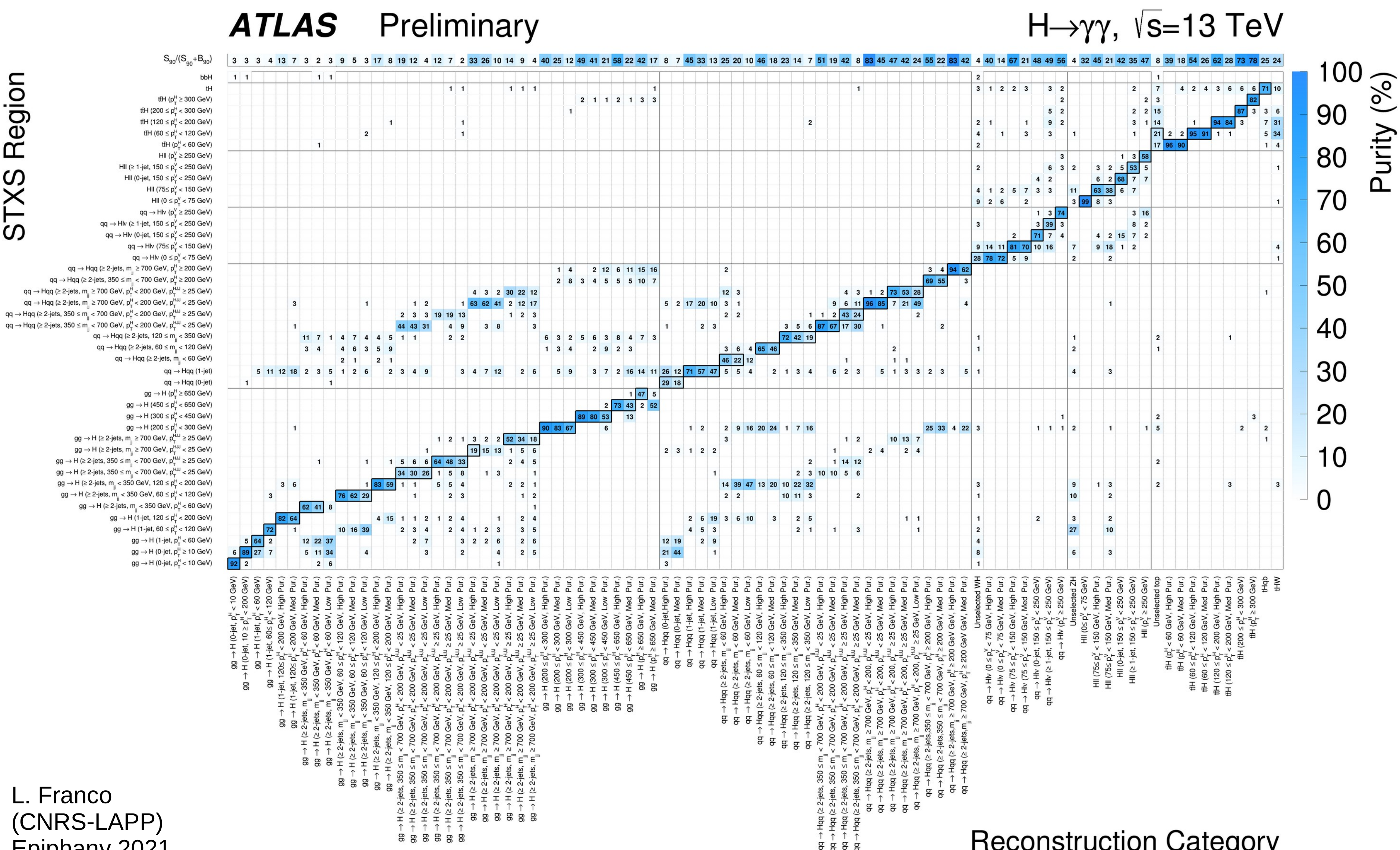

Signal modeling

- The signal is modeled with a Double sided Crystal Ball (DSCB) function: Gaussian core, power law tails;
- The DSCB is obtained by combining different signal MC according to the expected number of events.

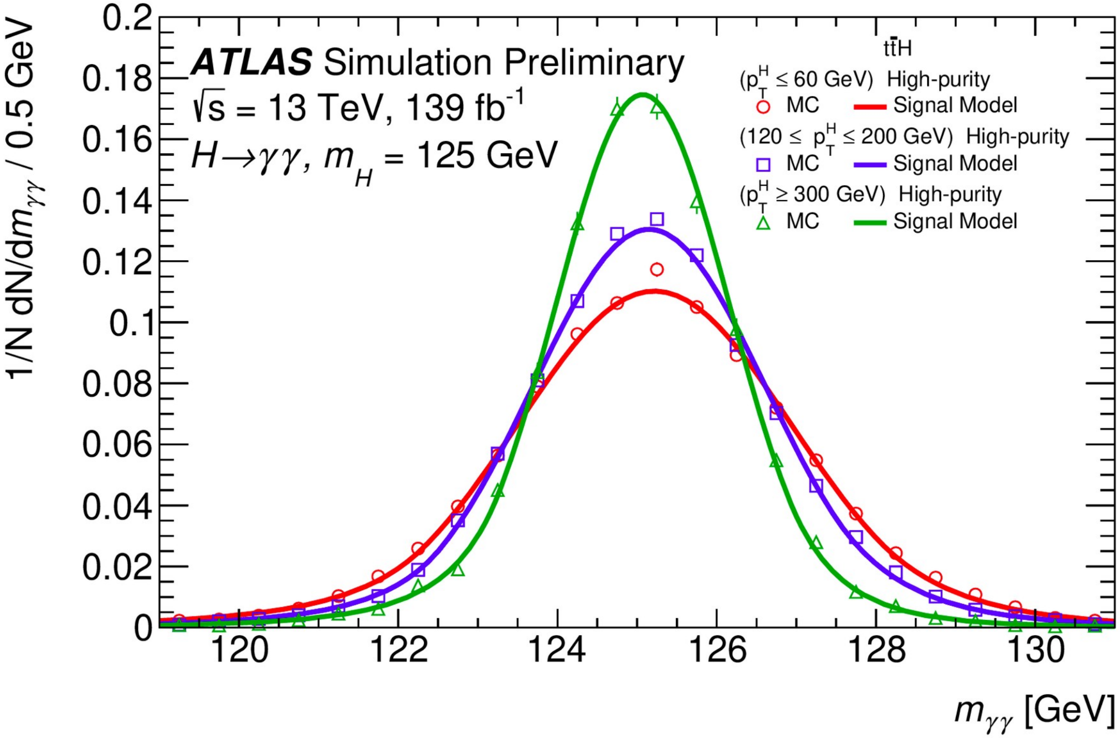

- DSCB is allowed to vary in the fit within the uncertainties coming from photon energy scale and resolution and Higgs boson mass measurements.

Background template construction

- For each gg→H and qq→Hqq category:
  - Estimate γ-jet, jet-jet components using data control regions;
  - Weight the γγ simulated sample to obtain $m_{\gamma\gamma}$ shape for the γ-jet and jet-jet components;
  - Combine according to their fractions to obtain the final template.
- For each VH, ttH and tH category:
  - Small contribution from γ-jet and jet-jet → neglected;
  - Template constructed using simulated processes (γγ, Vγγ, ttγγ) alone.

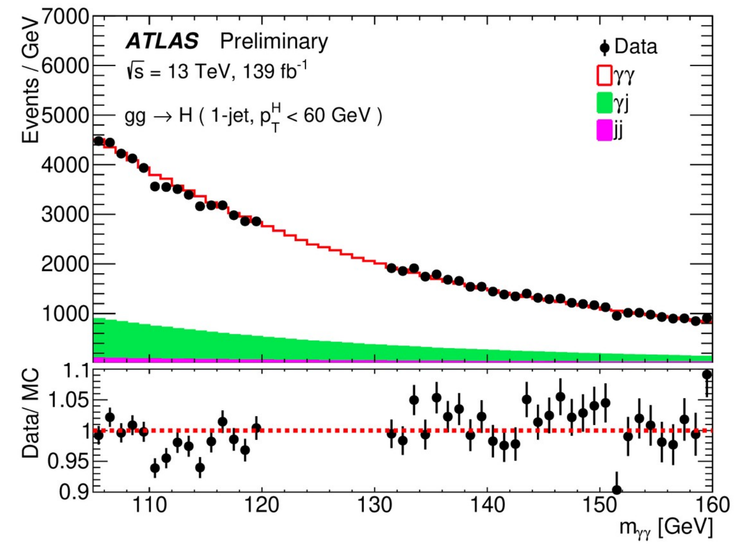

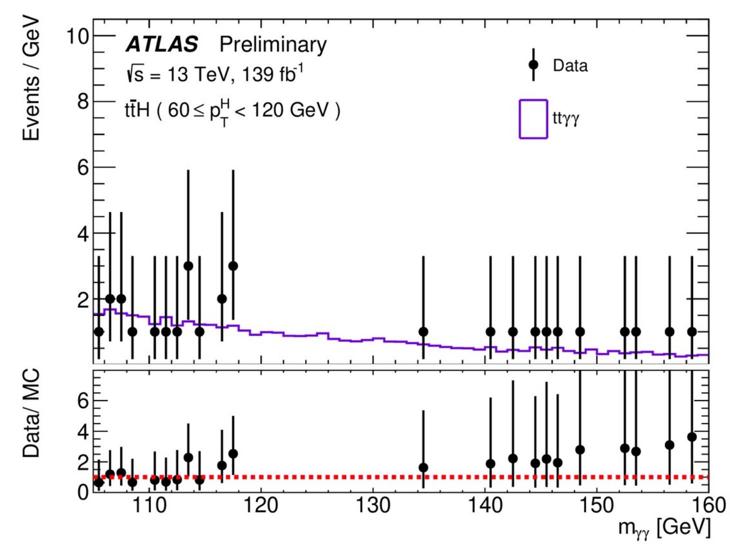

Choice of the background function

- Fitting template with Signal+Background PDF to estimate the possible bias induced by a mis-modeling of the background → this term is introduced for every category;
- For categories with high statistics (at least 100 events in data sidebands):
  - Choose the best candidate function that has minimum bias (according to spurious signal test).
- For categories with low statistics:
  - Consider only exponential-polynominal candidate functions;
  - Reject higher order exponential-polynominal functions according to a Wald test on data sidebands.
- The coefficients of these functions are free to float in the fit to the data.

Data sidebands: $m_{\gamma\gamma}$ in [105,120] or [130,160] GeV.

Type	Function	N_{pars}	Acronym
Power law	$m_{\gamma\gamma}^{a}$	1	PowerLaw
Exponential	$\exp(am_{\gamma\gamma})$	1	Exp
Exponential of second-order polynomial	$\exp(a_1 m_{\gamma\gamma} + a_2 m_{\gamma\gamma}^2)$	2	ExpPoly2
Exponential of third-order polynomial	$\exp(a_1 m_{\gamma\gamma} + a_2 m_{\gamma\gamma}^2 + a_3 m_{\gamma\gamma}^3)$	3	ExpPoly3
Bernstein polynomial	$(1-x)^n + a_1 nx(1-x)^{n-1} + \cdots + a_n x^n$	$n = 1$–5	Bern1–Bern5

STXS merging

- Not enough statistical power to fit all 44 → merge down to 27 bins.

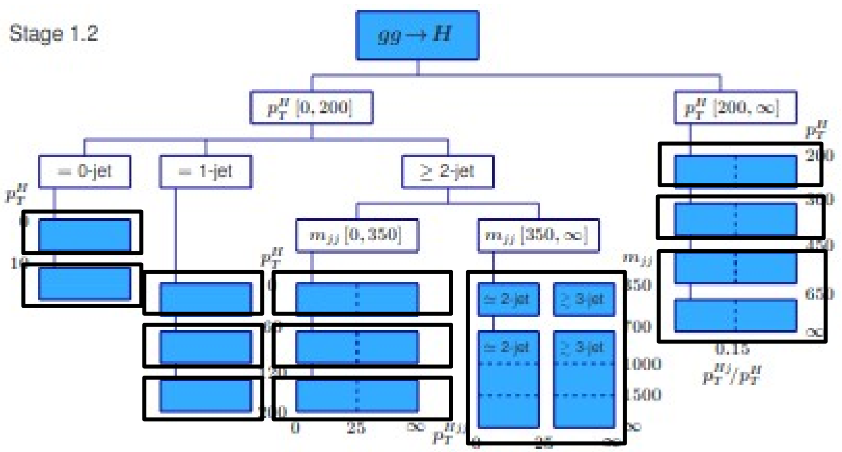

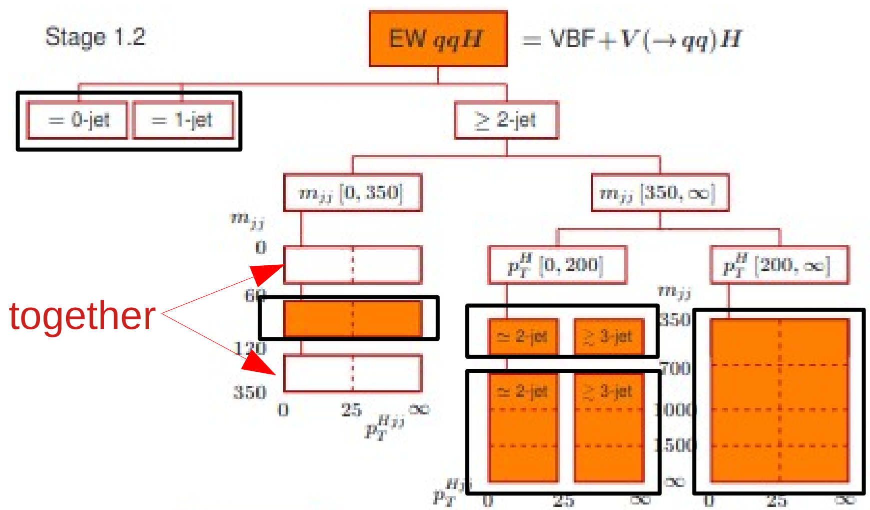

Merged together

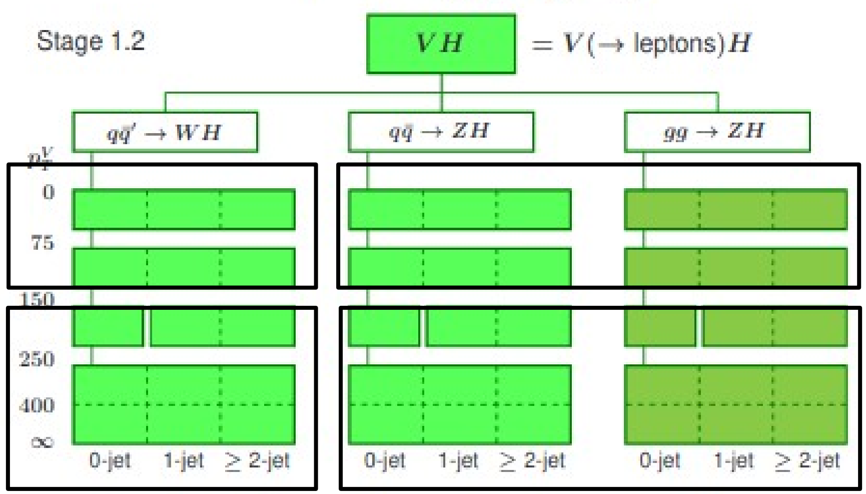

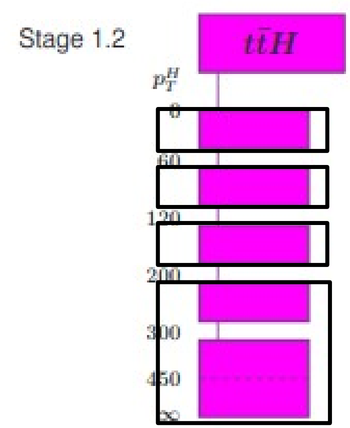

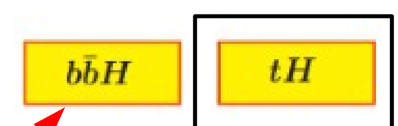

Merged to gg→H

Results: STXS

- Ratio to SM expectation is presented;
- Relative uncertainties from 20% to more than 100%;
- Upper limit of 8*SM prediction set on tH production;
- No significant deviation from the SM.

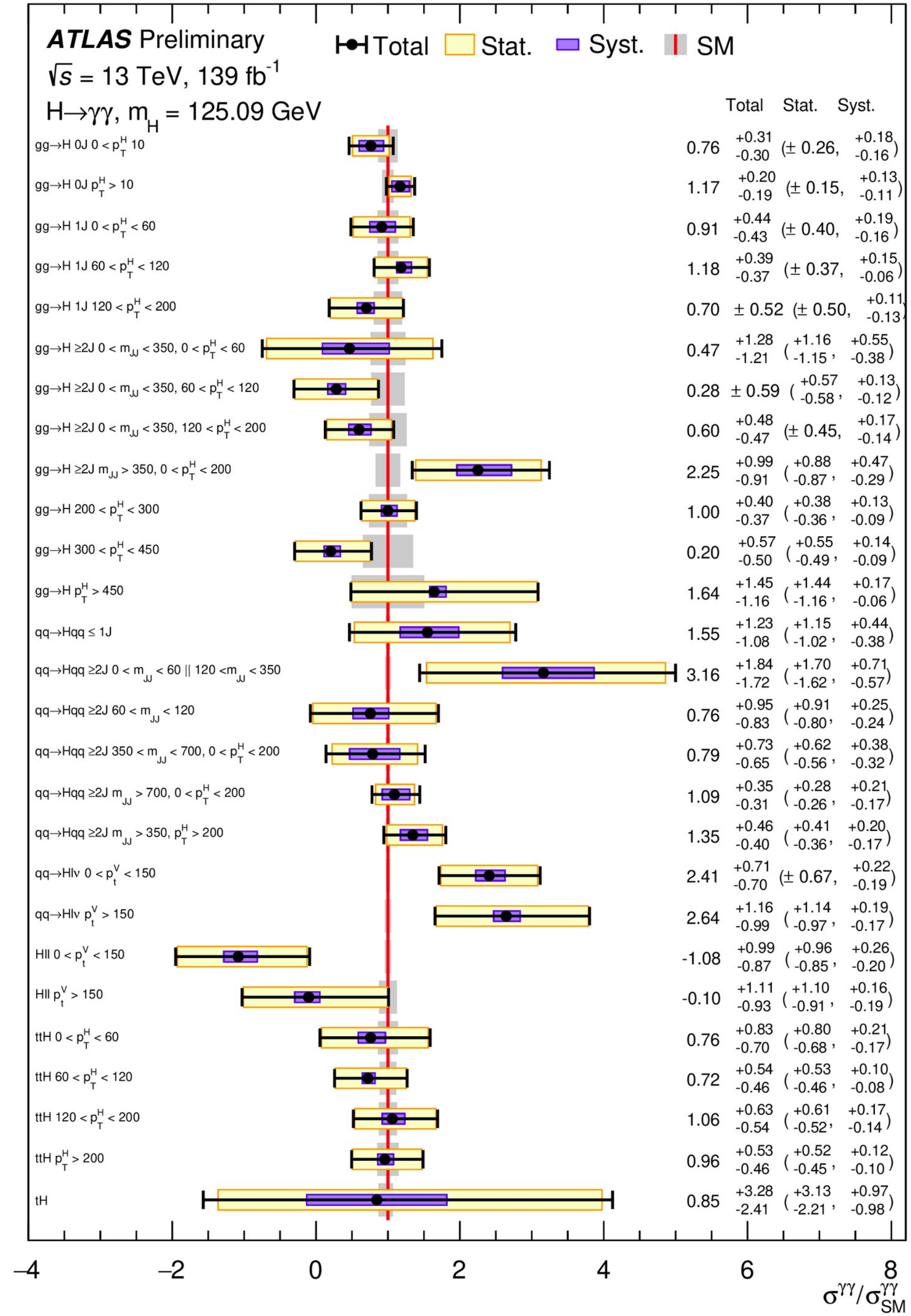

L. Franco
(CNRS-LAPP)
Epiphany 2021

Next step: EFT interpretation

- The SMEFT extends the SM Lagrangian by adding new operators;
- STXS are parametrized in terms of EFT coefficients;
- Find the set of c_i to which the dataset has maximum sensitivity;
- Constrain EFT coefficients → put limits on BSM theories.

$$\mathcal{L}_{\mathrm{EFT}} = \mathcal{L}_{\mathrm{SM}} + \sum_i \bar{c}_i^{(6)} O_i^{(6)}$$

Coefficient	Operator	Example process
c_{HDD}	$\left(H^\dagger D^\mu H\right)^* \left(H^\dagger D_\mu H\right)$	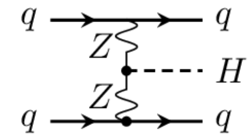
c_{HG}	$H^\dagger H\, G^A_{\mu\nu} G^{A\mu\nu}$	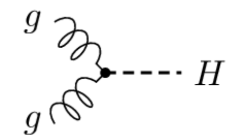
c_{HB}	$H^\dagger H\, B_{\mu\nu} B^{\mu\nu}$	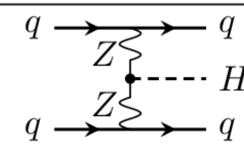
c_{HW}	$H^\dagger H\, W^I_{\mu\nu} W^{I\mu\nu}$	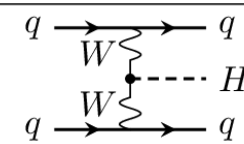
c_{HWB}	$H^\dagger \tau^I H\, W^I_{\mu\nu} B^{\mu\nu}$	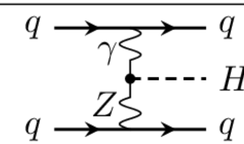
c_{eH}	$(H^\dagger H)(\bar{l}_p e_r H)$	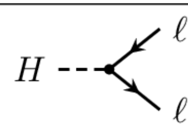
$c^{(1)}_{Hl}$	$(H^\dagger i \overleftrightarrow{D}_\mu H)(\bar{l}_p \gamma^\mu l_r)$	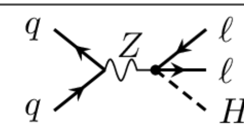
c_{uG}	$(\bar{q}_p \sigma^{\mu\nu} T^A u_r)\widetilde{H}\, G^A_{\mu\nu}$	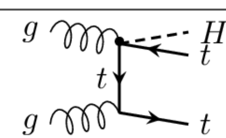
c_{uW} c_{uB}	$(\bar{q}_p \sigma^{\mu\nu} u_r)\tau^I \widetilde{H}\, W^I_{\mu\nu}$ $(\bar{q}_p \sigma^{\mu\nu} u_r)\widetilde{H}\, B_{\mu\nu}$	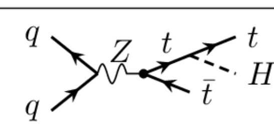

Red circles: H→γγ is the most sensitive

EFT results from Higgs combination

- Combination of H→γγ, H→bb (VH only), H→ZZ*→4l analyses;
- Results published by the collaboration in ATLAS-CONF-2020-053;
- Measuring combination of c_i to which we are most sensitive;
- SMEFT linearized model and model including quadratic terms;
- No significant deviation from the SM.

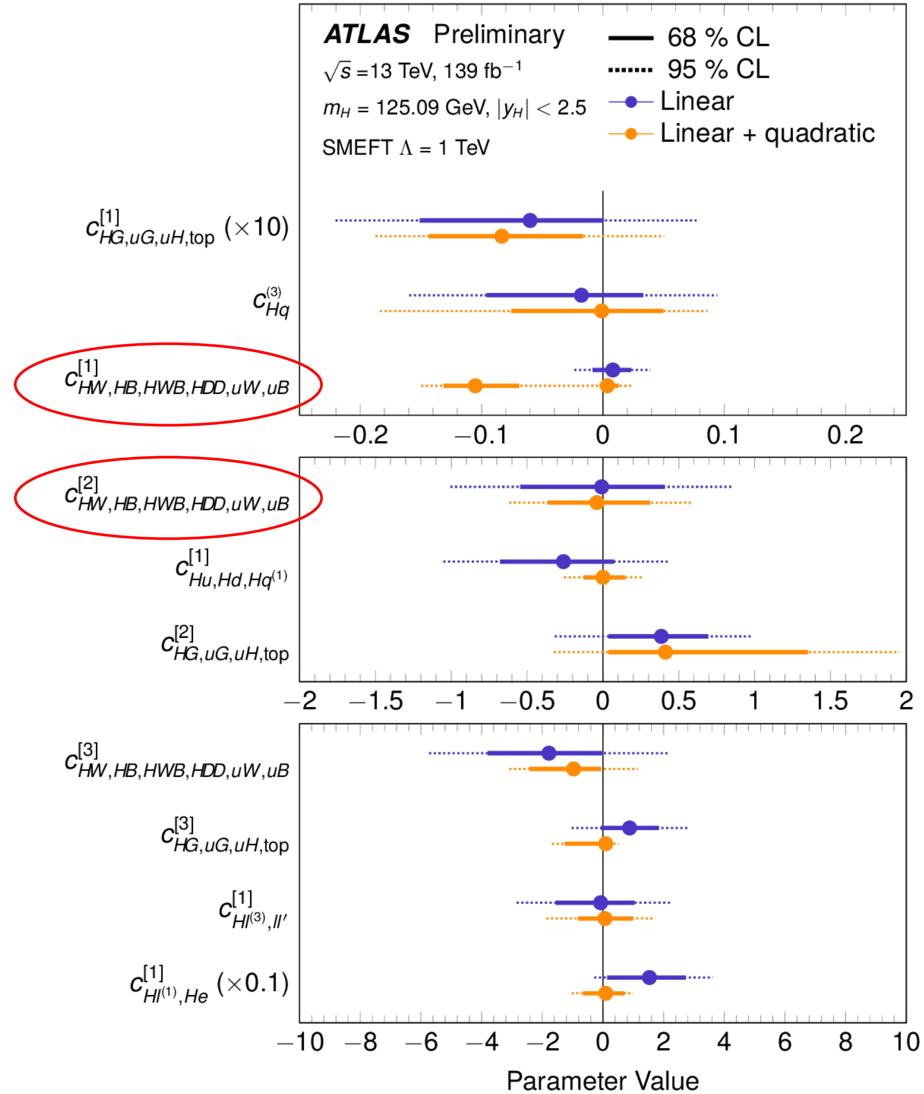

H→γγ leading the sensitivity

Conclusions

- Measurements of the properties of the Higgs boson production at $\sqrt{s}$=13 TeV in the diphoton decay channel;
- STXS results of the combination with other decay channels interpreted through EFT;
- Legacy paper foreseen in 2021 with improvements:
  - New categorization → to reduce correlation between ZH and WH;
  - Background smoothing → to reduce spurious signal bias;
  - H→γγ standalone interpretation with EFT and kappa frameworks.
- Very important test for the SM prediction → no hint of new physics observed.

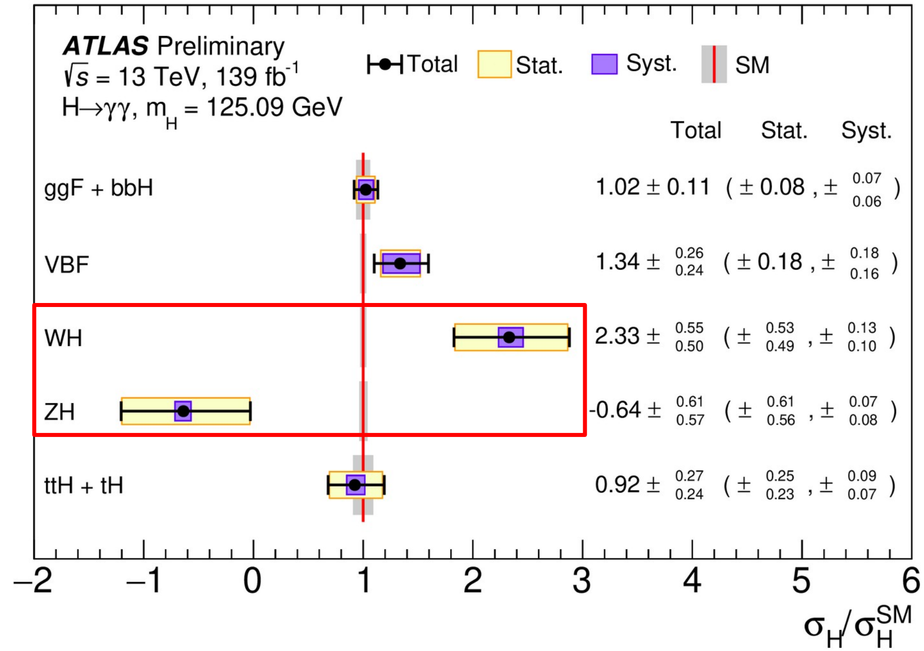

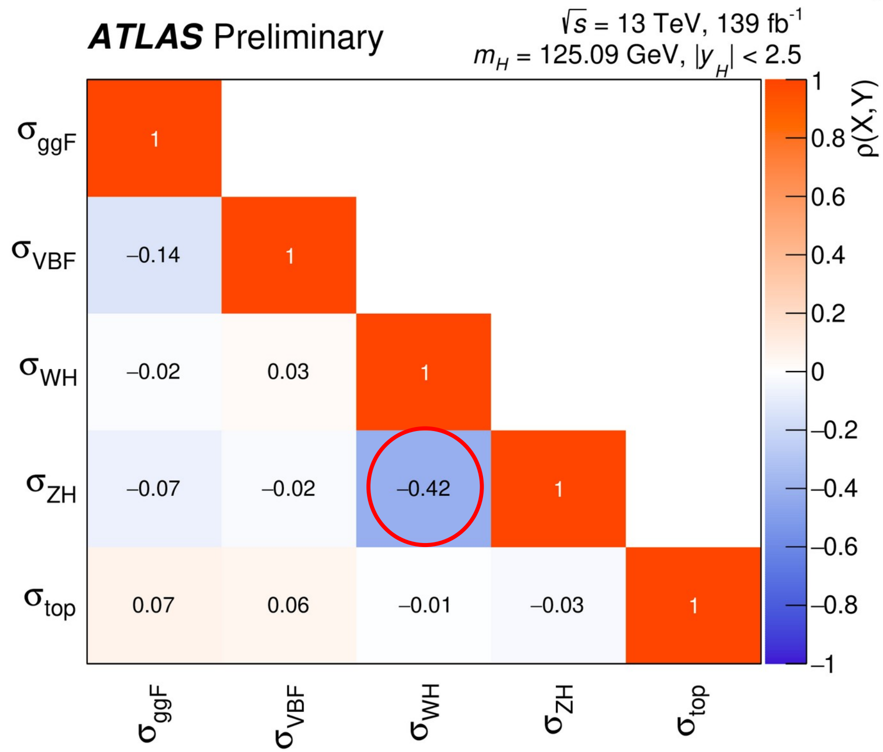

L. Franco
(CNRS-LAPP)
Epiphany 2021

BACK-UP

Event selection

- Reconstructed photon candidates must satisfy a preselection:
  - p_T>25 GeV;
  - $|\eta|<2.37$ (with $1.37<|\eta|<1.52$ excluded);
  - Loose identification requirement;
- Diphoton selection:
  - Two highest p_T preselected photons;
  - Vertex selected using a Neural Network;
- Final event selection:
  - Tight identification requirement and well isolated photons;
  - $p_T^{\gamma 1}/m_{\gamma\gamma}>0.35$ and $p_T^{\gamma 2}/m_{\gamma\gamma}>0.25$
  - $105 < m_{\gamma\gamma} < 160$ GeV

Categorization: summary

- IDEA: Targets the full STXS granularity simultaneously. Optimized for the determinant of the covariance matrix of the results, it takes into accounts both errors and correlations of the fit.
- PROCEDURE:
  - Train a multiclass BDT over 44 STXS truth bins (signal only) with high level and top-reco variables;
  - D-optimality: weight the multiclass outputs and classify events in 44 reco classes;
  - In each reco class, train a binary BDT (signal vs backgrounds) with high level and top-reco variables;
  - Build 88 categories with significance scans over BDT outputs

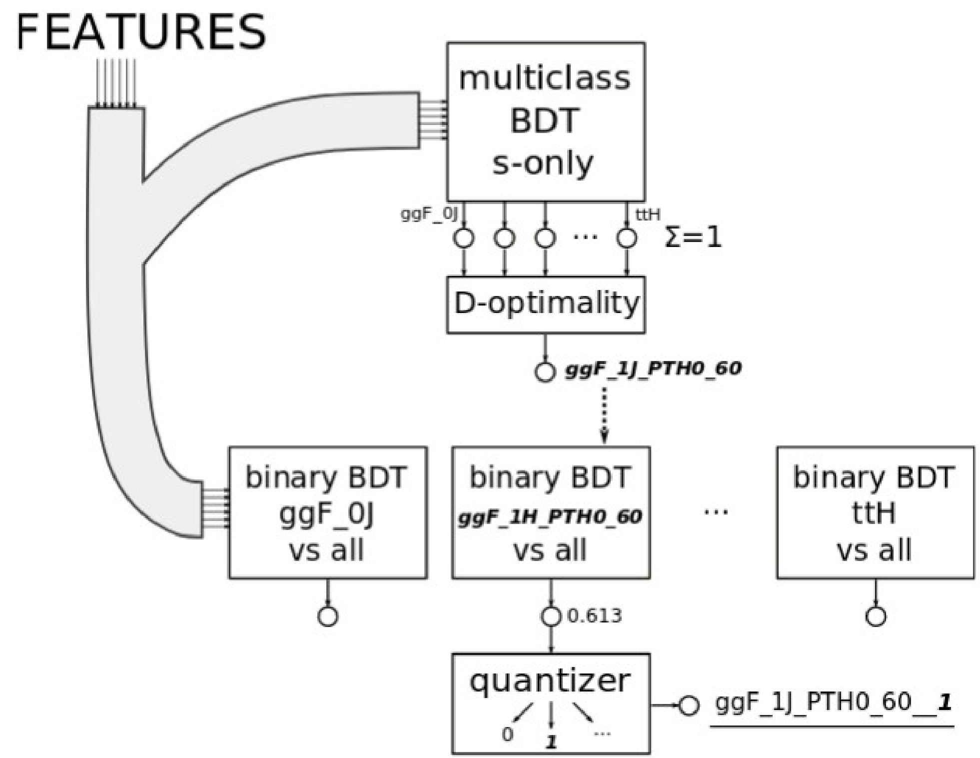

Categorization purity: gg→H

- Correspondence between gg→H STXS bins and reconstructed categories targeting them.

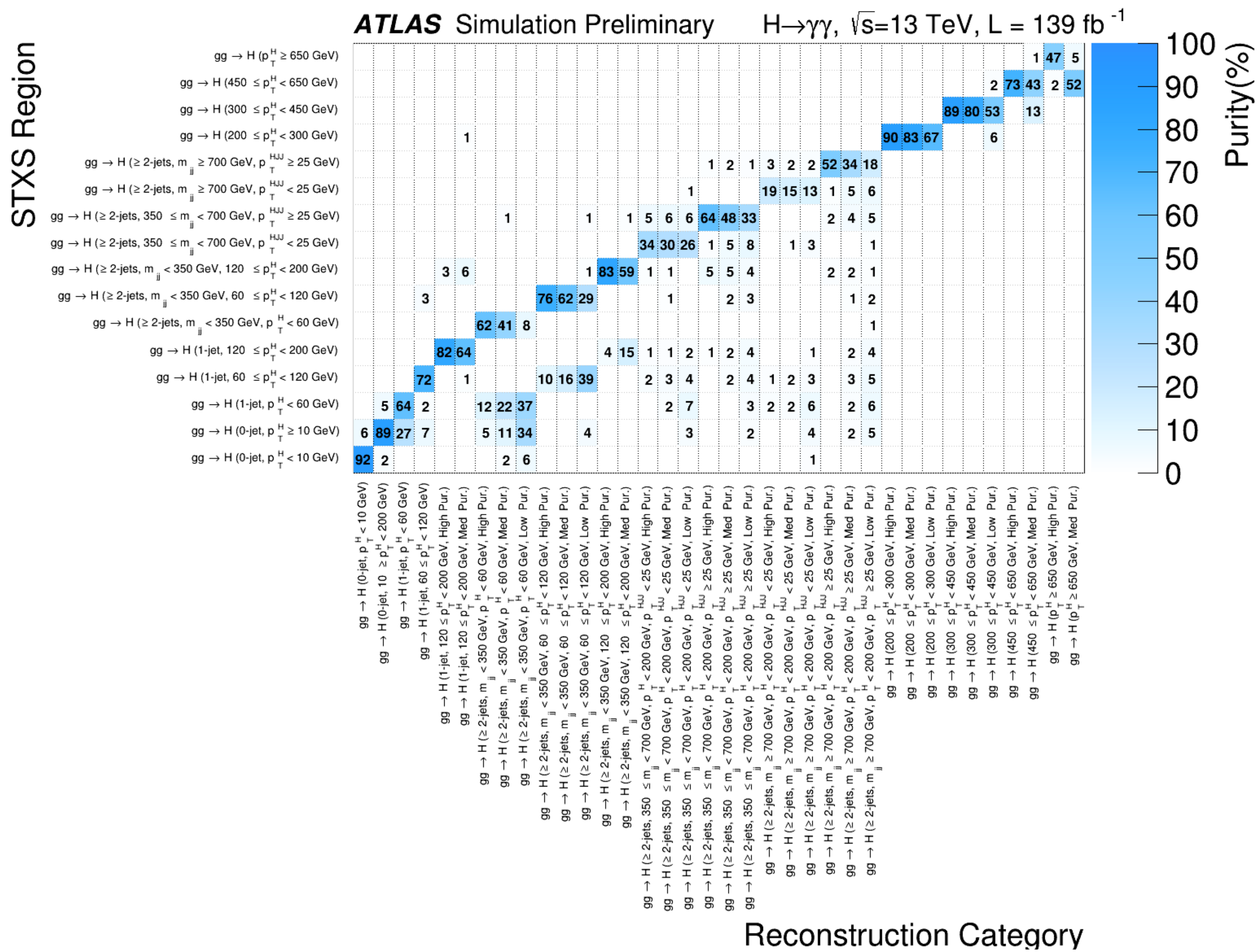

Categorization purity: qq→Hqq

- Correspondence between qq→Hqq STXS bins and reconstructed categories targeting them.

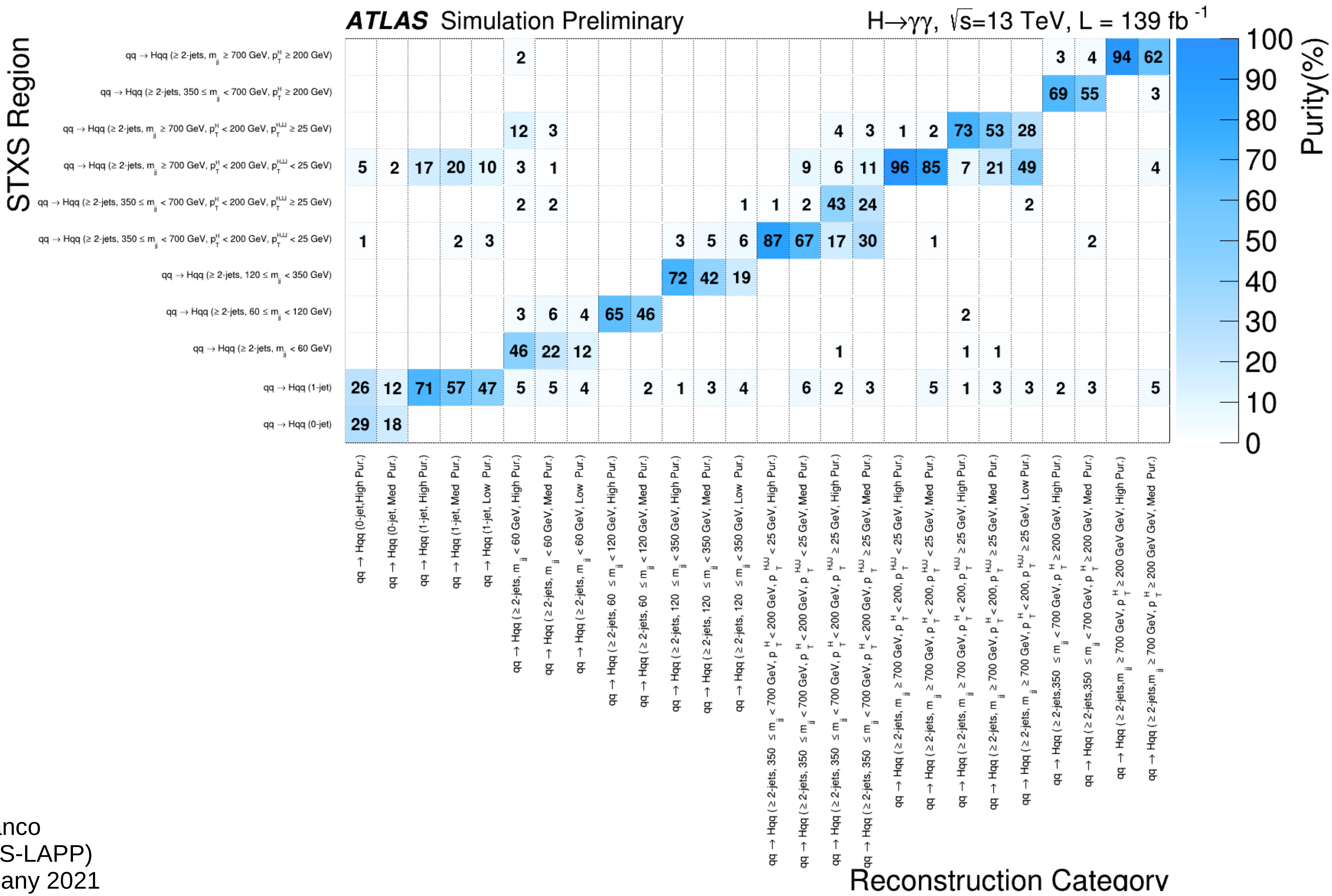

L. Franco
(CNRS-LAPP)

Categorization purity: ttH, tH

- Correspondence between ttH, tH STXS bins and reconstructed categories targeting them.

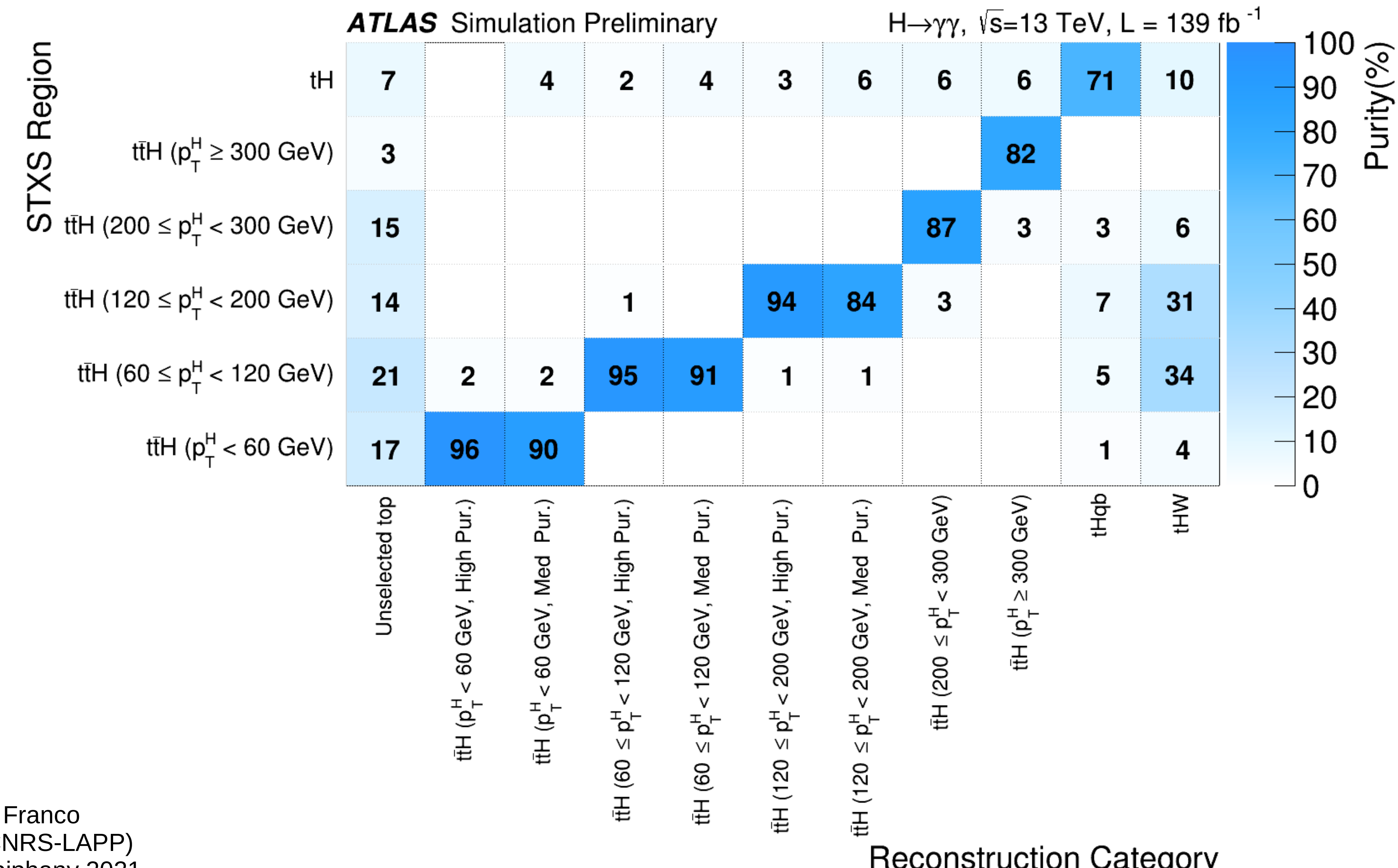

Categorization purity: migrations

- Correspondence between qq→Hqq STXS bins and reconstructed categories targeting gg→H.

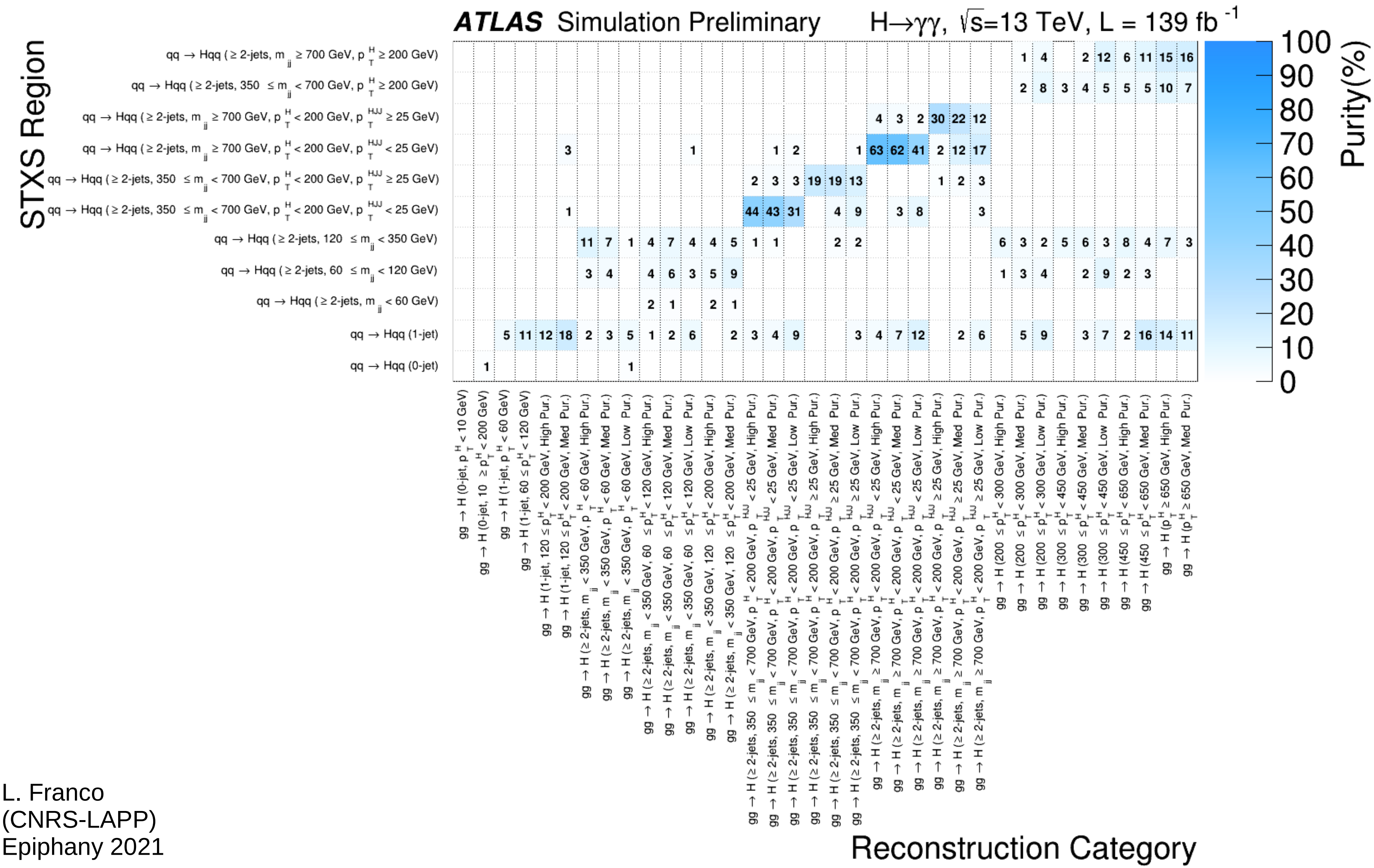

L. Franco
(CNRS-LAPP)
Epiphany 2021

Categorization purity: migrations

- Correspondence between gg→H STXS bins and reconstructed categories targeting qq→Hqq.

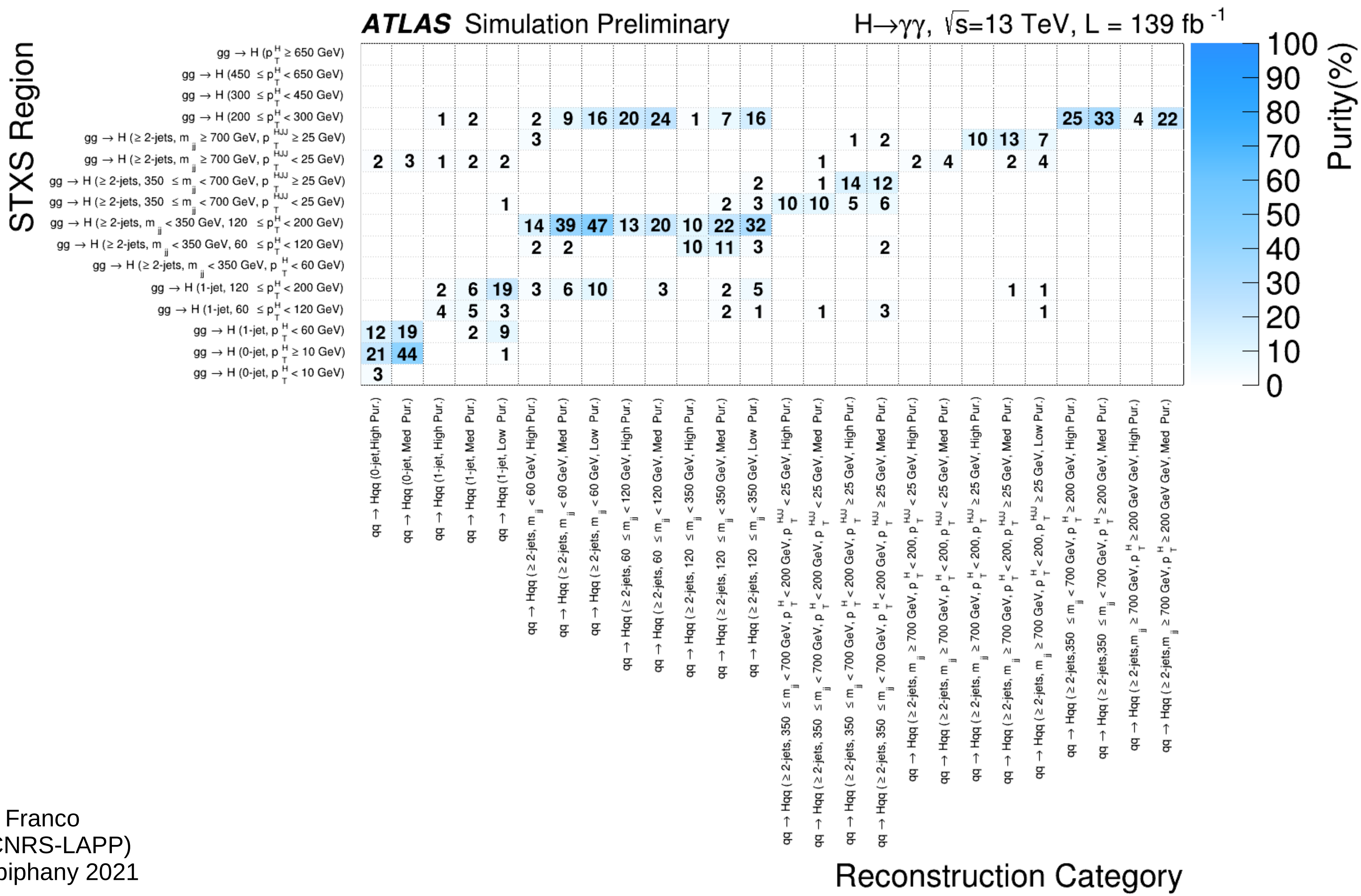

L. Franco
(CNRS-LAPP)
Epiphany 2021

Background modeling: summary

- Construct background templates using MC or data control regions;
- Fit the obtained templates with a set of functions, choose the one that:
  - Gives the smallest bias (spurious signal test);
  - Doesn't overfit the template (Wald test).

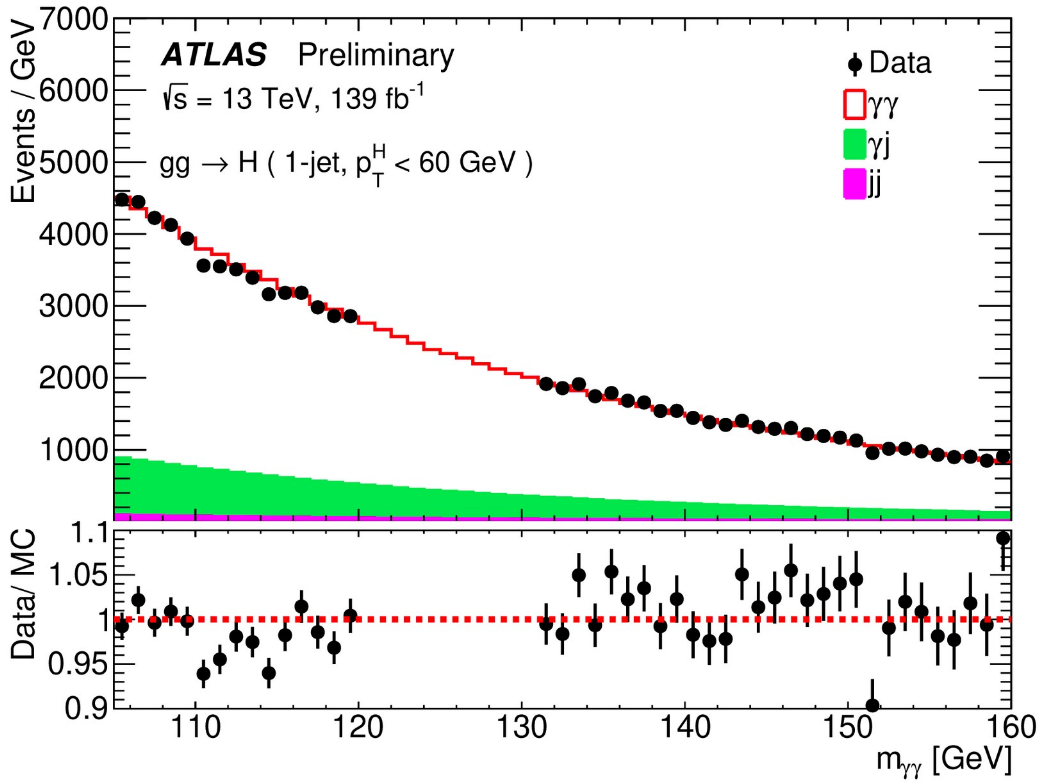

Spurious signal test

- In each category, a signal+background fit is performed over the background-only template and the value of the fitted signal yield S_{spur} is reported;
- Each candidate function is tested independently;
- The function passes the test if:
  - $|S_{spur}| <$ 10% of expected signal yield;
  - Or $|S_{spur}| <$ 20% of the statistical uncertainty of the fitted (expected) signal yield.
- Additionally, the fit is required to bring a χ^2 probability of at least 1%;
- If more than one candidate passes for a category, the one with less degrees of freedom is chosen.

Type	Function	N_{pars}	Acronym
Power law	$m_{\gamma\gamma}^{a}$	1	PowerLaw
Exponential	$\exp(a m_{\gamma\gamma})$	1	Exp
Exponential of second-order polynomial	$\exp(a_1 m_{\gamma\gamma} + a_2 m_{\gamma\gamma}^2)$	2	ExpPoly2
Exponential of third-order polynomial	$\exp(a_1 m_{\gamma\gamma} + a_2 m_{\gamma\gamma}^2 + a_3 m_{\gamma\gamma}^3)$	3	ExpPoly3
Bernstein polynomial	$(1-x)^n + a_1 n x (1-x)^{n-1} + \cdots + a_n x^n$	$n = 1$–5	Bern1–Bern5

Wald test

- For categories with less than 100 data events in the control region, a Wald test is performed in order to choose the analytical function modeling the background in the category;
- Candidate background functions are limited to Exp,ExpPoly2 and ExpPoly3, in order to avoid unphysical fits due to large statistical fluctuations;
- The quantity q_{12} is computed, where L_1 and L_2 are the maximum likelihood values corresponding to the use of Exp and ExpPoly2 in the fit;
- The ExpPoly2 model is chosen if the p-value associated to q_{12} is less than 0.05;
- Similarly, the ExpPoly3 form is chosen over ExpPoly2if the p-value for the corresponding Wald test is 0.05 or less.

$$q_{12} = -2 \log \frac{L_1}{L_2}$$

STXS observed correlations

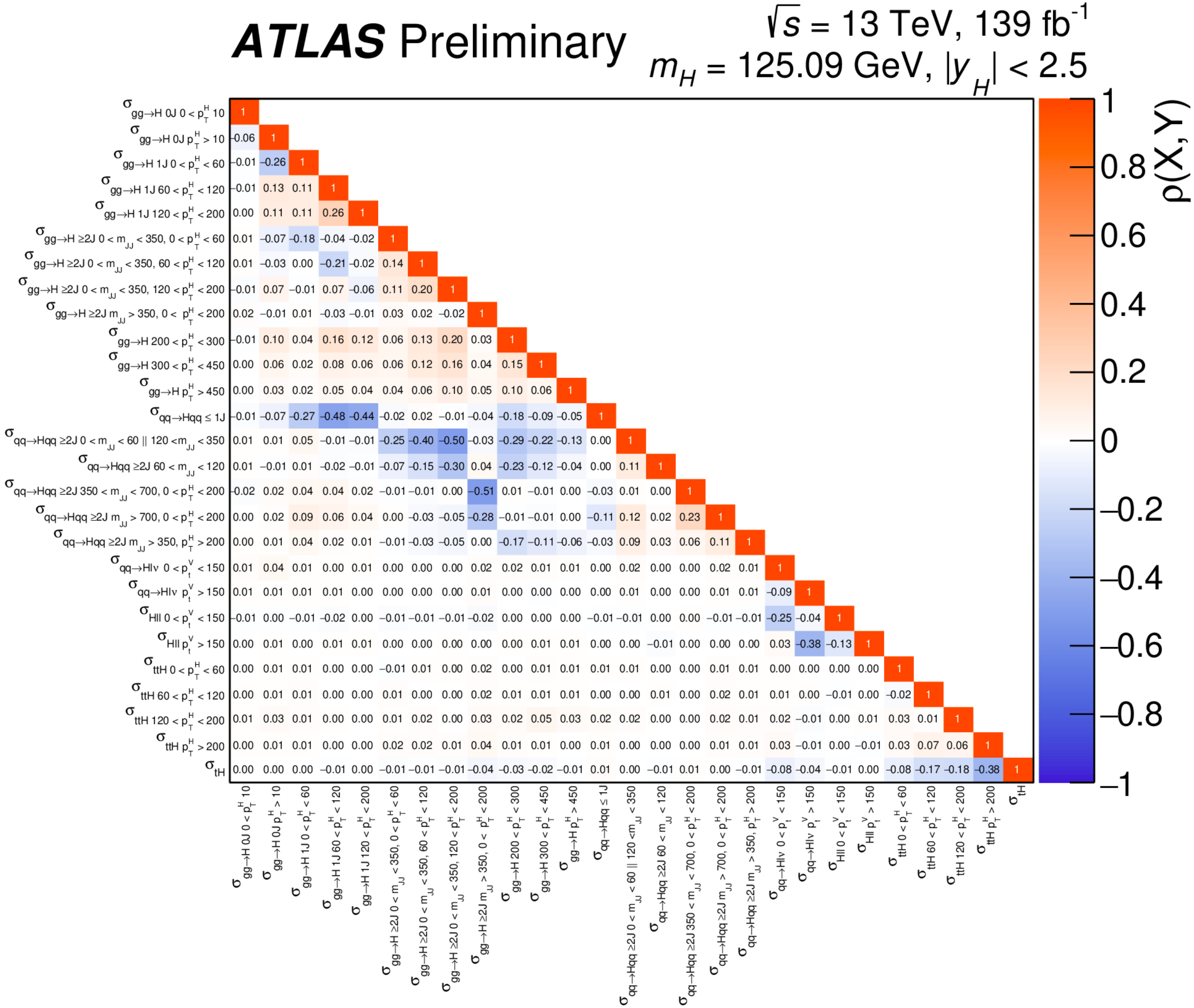

Results: Production mode XS

- Production modes xs are measured;
- Ratio to SM expectation is presented;
- Smaller (larger) than expected yield for ZH (WH);
- -42% correlation between ZH and WH;
- Good compatibility with the SM (p-value of 3%).

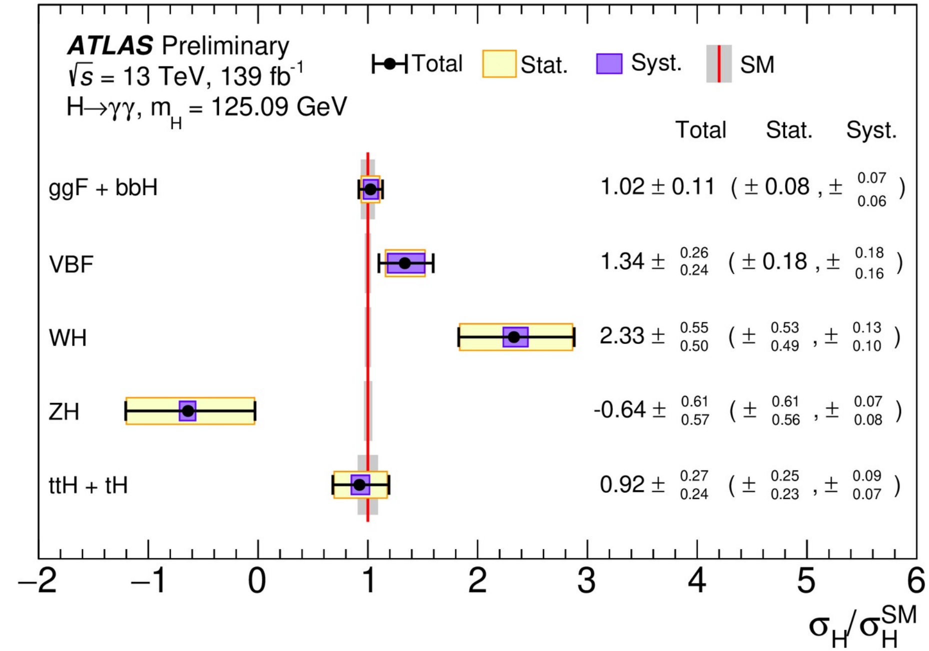

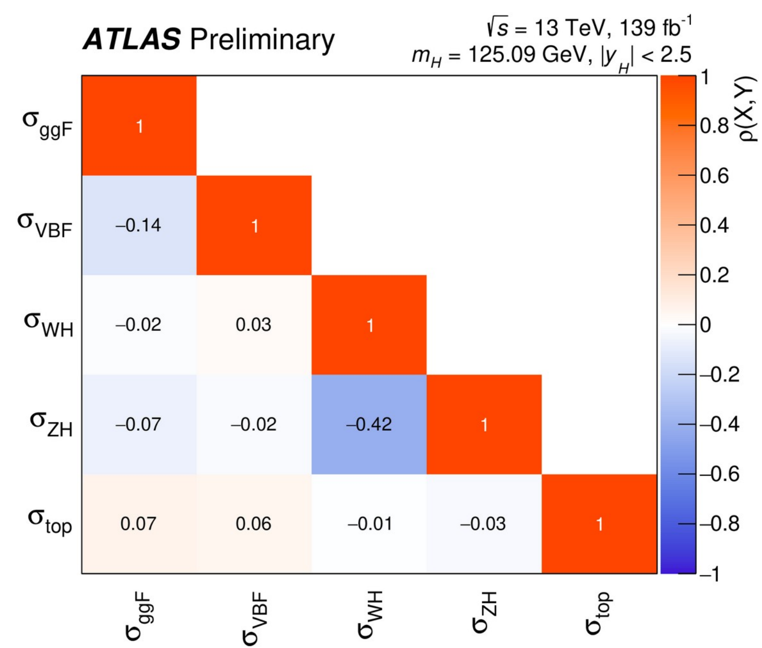

L. Franco
(CNRS-LAPP)
Epiphany 2021

Main systematics

- Theoretical: perturbative QCD calculations, modeling of parton shower, choices of the parton distribution functions and value of alphaS, modeling of heavy flavor quark production in non-ttH processes.
- Experimental (shape): photon energy scale (<0.3%) and resolution (between 1% and 8%);
- Experimental (yield): Among many, the uncertainties with the largest variations in signal yields are the pileup modeling uncertainty(up to 7%), jet flavor tagging uncertainty (up to 5%), and jet energy resolution uncertainty (up to 4%).
- Background modeling: Bias induced by the choice of the analytical function (spurious signal) range from 10% to 99% of the stat uncertainty in that category.

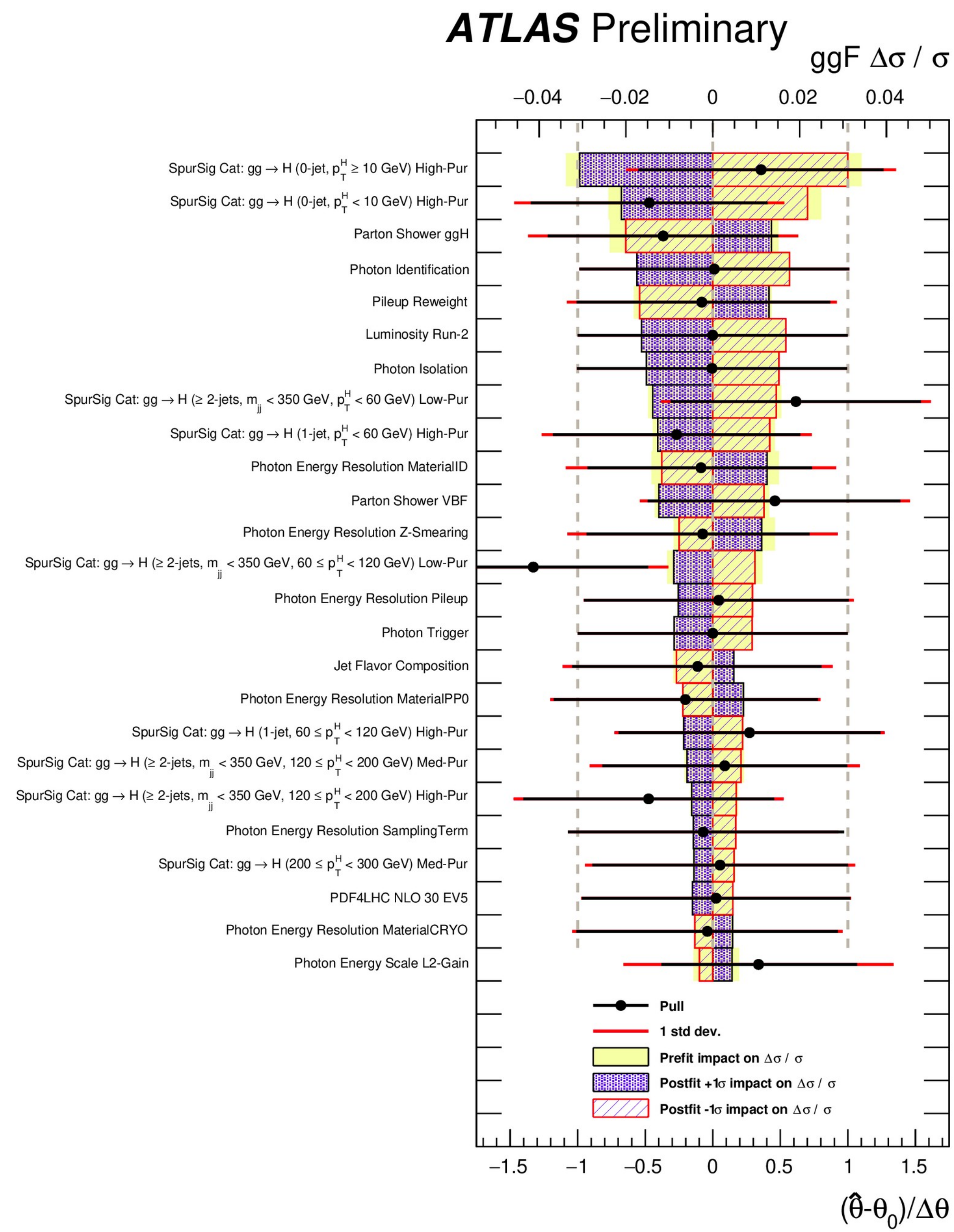

EFT: choice of measured parameters

- It's not possible to fit/constrain all the c_i → must find the optimal set through a Principal Component Analysis;
- C_{STXS} is the SM expected covariance matrix of the measurement; P is the linearised parametrisation matrix;
- C^{-1}_{EFT} represents (Gaussian approx.) the Fisher information matrix of its SMEFT re-parametrisation;
- Eigenvalue decomposition of C^{-1}_{EFT} → eigenvectors corresponding to the most sensitive directions.

ATLAS Preliminary $\sqrt{s}$ =13 TeV, 139 fb^{-1}

$$C^{-1}_{\mathrm{EFT}} = P^{\top} C^{-1}_{\mathrm{STXS}} P$$

#	λ	$c_{Hq}^{(3)}$	c_{HB}	c_{HW}	c_{HWB}	c_{uB}	c_{uW}	c_{HDD}	c_{Hd}	c_{Hu}	$c_{Hq}^{(1)}$	c_{He}	$c_{Hl}^{(1)}$	$c_{Hl}^{(3)}$	c'_{ll}	c_{HG}	c_{uG}
1	299310		-0.70	-0.23	0.39	-0.04	-0.02									0.55	0.02
2	121830		-0.47	-0.15	0.26	-0.03										-0.83	-0.03
3	1960	0.99		0.10	0.03				-0.03	0.09	-0.05			-0.02	0.02		
4	38	-0.11	0.09		0.15			0.02	-0.26	0.84	-0.41	-0.02	-0.02	-0.06	0.04		0.08
5	19		0.10	-0.19	0.06					0.03	-0.02	-0.07	0.09	-0.13	0.10	0.02	-0.69
6	10	0.08		-0.57	-0.34			-0.02	-0.02	0.08	-0.10	0.13	-0.13	0.54	-0.40		-0.04
7	5.9	-0.07	-0.23	0.73		-0.03	-0.02	-0.03	-0.02	0.08		0.10	-0.15	0.44	-0.25		-0.13
8	1.1	-0.01	-0.02	0.08				-0.02	-0.02	0.04	-0.02	-0.01	0.02	0.08	-0.03	0.03	-0.68
9	0.3	-0.02	-0.41	0.09	-0.70	-0.02	-0.01	-0.12	0.01	-0.03	-0.36	0.16		-0.37	0.10		-0.05
10	0.16		0.09	-0.09	0.09	-0.04	-0.01	-0.04		0.10	0.31	0.29	-0.58	-0.26	-0.12		-0.07
11	0.036		0.03	0.03	0.07	-0.01	0.04	0.19	-0.04		0.03	0.09	-0.06	-0.18	-0.07	0.01	-0.16
12	0.023		-0.01				0.37	-0.01		-0.01	-0.03	-0.02	0.03	0.05	0.03		0.01

#	λ	c_G	$c_{qd}^{(8)}$	$c_{qq}^{(1)}$	c_{qq}	$c_{qq}^{(3)}$	$c_{qq}^{(31)}$	$c_{qu}^{(1)}$	$c_{qu}^{(8)}$	c_{uH}	$c_{ud}^{(8)}$	c_{uu}	$c_{uu}^{(1)}$	$c_{H\Box}$	c_{dH}	c_W	c_{eH}
1	299310															-0.02	
2	121830																
3	1960																
4	38									0.02				0.03			
5	19	0.17	0.03	0.03	0.22	0.05	0.52		0.15	-0.08	0.03	0.02	0.23	0.07	0.06		
6	10				0.02		0.04			-0.02			0.02	-0.20	-0.08		
7	5.9	0.08			0.09	0.02	0.22		0.06				0.10	-0.07	-0.11		
8	1.1	-0.29	-0.03	-0.04	-0.24	-0.04	-0.52	-0.01	-0.15	-0.10	-0.03	-0.02	-0.25	0.04			
9	0.3	0.03								0.06				0.06	-0.11	-0.01	
10	0.16	0.02				-0.04				0.08				0.27	-0.52	-0.02	0.01
11	0.036	0.22	-0.01	0.01	-0.01	-0.10	-0.09		-0.02	0.70	-0.01		-0.02	-0.56	0.09		-0.02
12	0.023	-0.05			0.03	-0.91	0.08		0.02	-0.02			0.03	0.09			